compositions by using ethylenediamine, added to the synthesis gel, as a template. The structure is constructed from two distinct elements of structure. These are sheets containing alternating tetrahedra joined to produce four-membered and elliptical eight-membered rings and slabs composed of trigonal-bipyramidal tetramers cross-linked by PO_4 tetrahedra. These units, infinite in (100), alternate along *a*. By way of comparison, frameworks 21 and EN3[8] are composed of corrugated sheets containing 5-coordinated aluminum between which run chains (crankshafts in the case of type 21; zigzag for type EN3) of alternating AlO_4 and PO_4 tetrahedra.[5,8] This class of open frameworks contains elements of structures containing only alternating tetrahedra (analogous to the zeolites) and those dense phases containing no 4-coordinate aluminum (or gallium) such as $AlPO_4$-15.[3,16] One feature not shared with the class by type 12 is a protonated framework. All protons reside on the amine with the framework carrying two negative charges, leading to the formula $[(MPO_4)(M_2P_2O_9^{2-})(N_2C_2H_{10}^{2+})]$. The dehydration of the framework, to produce a four-connected all-tetrahedral net, is not likely. Such a dehydration does occur for type 21 to produce type 25, a molecular sieve with eight-membered-ring apertures.

The only significant differences between $AlPO_4$-12 and $GaPO_4$-12 concern the geometry of the Ga- and Al-centered polyhedra.

Acknowledgment. Most of this work was undertaken at The Research School of Chemistry. For the support given by the school's staff I am most grateful.

Registry No. $AlPO_4$-12(en), 98218-54-3; $GaPO_4$-12(en), 98218-56-5; Al_2O_3, 1344-28-1; Ga_2O_3, 12024-21-4; H_3PO_4, 7664-38-2; en, 107-15-3.

Supplementary Material Available: Tables of anisotropic thermal parameters, details of hydrogen bonds, and structure factors (26 pages). Ordering information is given on any current masthead page.

Contribution from the Department of Chemistry, University of British Columbia, Vancouver, B.C., Canada V6T 1Y6

Synthesis, Stability, and Fluxional Behavior of Binuclear Mixed-Hydride–Tetrahydroborate Complexes of Hafnium(IV): X-ray Crystal Structure of $[[(Me_2PCH_2SiMe_2)_2N]Hf(BH_4)_2](\mu\text{-}H)_3[Hf(BH_4)[N(SiMe_2CH_2PMe_2)_2]]$

MICHAEL D. FRYZUK,*[1a] STEVEN J. RETTIG,[1b] AXEL WESTERHAUS, and HUGH D. WILLIAMS

Received March 19, 1985

Addition of PMe_3 to the mononuclear tris(tetrahydroborate) complex of hafnium $Hf(BH_4)_3[N(SiMe_2CH_2PMe_2)_2]$ (**4**) results in the formation of the binuclear mixed-hydride–tetrahydroborate derivative $[Hf[N(SiMe_2CH_2PMe_2)_2]]_2(\mu\text{-}H)_3(BH_4)_3$ (**6**). The X-ray data for **6** are as follows: triclinic, space group $P\bar{1}$; a = 13.333 (3), b = 18.722 (3), and c = 9.690 (3) Å; α = 94.02 (2), β = 107.04 (2), and γ = 109.14 (2)°; V = 2147 Å^3; Z = 2; R = 0.042 and R_w = 0.057 for 7675 reflections with $I \geq 3\sigma(I)$ from 9827 unique reflections using 328 variables; μ(Mo Kα) = 50.6 cm^{-1}. The solid-state structure shows three bridging hydrides between the two hafnium centers and three different BH_4^- ligands: one bound in a tridentate fashion to one hafnium and the remaining two BH_4^- units bound to the other hafnium in a bidentate mode and a distorted monodentate mode of attachment. To explain the simple ^1H and $^{31}P\{^1H\}$ NMR spectra, it is proposed that an intramolecular BH_4^- migration from one hafnium to the other occurs in the fast-exchange limit. Addition of excess NMe_3 to **4** or **6** results in further BH_3 cleavage to generate the binuclear tetrahydride $[Hf[N(SiMe_2CH_2PMe_2)_2]]_2(\mu\text{-}H)_4(BH_4)_2$ (**7**). The solution spectroscopic data are consistent with fast rotation of the ends of the dimer on the NMR time scale; an activation barrier of 13.4 kcal mol^{-1} was calculated for this rotational process. On the basis of product analysis and deuterium-labeling studies, a mechanism for the formation of these binuclear mixed-hydride–tetrahydroborate complexes is proposed that involves fragmentation of the unstable binuclear intermediate $[Hf[N(SiMe_2CH_2PMe_2)_2]]_2(\mu\text{-}H)_2(BH_4)_4$ followed by recombination; simple BH_3 cleavage is not involved.

Transition-metal complexes containing metal–hydride bonds are implicated in many stoichiometric and catalytic organic transformations.[2] For this reason, the synthesis, structural characterization, and chemical behavior of new metal–hydride complexes continues to be an endeavor of numerous research groups.[3]

It is now well established that hydride complexes of the group 4 transition metals, specifically zirconium and hafnium, offer reactivity patterns that are more comparable to boron or aluminum hydrides than to some of the "later"-transition-metal–hydride complexes.[4,5] However, the vast majority of the known group 4 metal hydrides contain cyclopentadienyl or substituted-cyclopentadienyl groups as ancillary ligands (e.g. $[(\eta^5\text{-}C_5H_5)_2Zr(H)Cl]_x$,[6] $[(\eta^5\text{-}C_5H_4Me)_2ZrH_2]_2$,[7] and $(\eta^5\text{-}C_5Me_5)_2ZrH_2$[8]). If the reactivity of a given transition-metal complex can be fine tuned to some extent by modifying these ancillary ligands, then donor types other than cyclopentadienyl must be investigated to expand the potentially rich chemistry of this particular group.

We have recently[9,10] devised a strategy whereby *soft* donors, such as phosphines, can form stable adducts with the *hard* metal centers, Zr(IV) and Hf(IV). The apparent mismatching[11] of *hard–soft* pairs is overcome by incorporating the *soft* donors into a chelating array (as in **1**) that also contains a *hard* donor such as an amide ligand, $^-NR_2$ (R = alkyl or silyl); since amides of Zr(IV) and Hf(IV) are known[12] to be stable, the tendency for

(1) (a) Fellow of the Alfred P. Sloan Foundation (1984–1986). (b) Experimental Officer, UBC Crystal Structure Service.
(2) Collman, J. P.; Hegedus, L. S. "Principles and Applications of Organotransition Metal Chemistry"; University Science Books: Mill Valley, CA, 1980; Chapters 3.3, 4.1, 5.1, 6, and 7.
(3) (a) Bau, R., Ed. "Transition Metal Hydrides"; American Chemical Society: Washington, DC, 1978; Adv. Chem. Ser. No. 167. (b) Toogood, G. E.; Wallbridge, M. G. H. *Adv. Inorg. Chem. Radiochem.* **1982**, *25*, 67. (c) Mayer, J. M.; Bercaw, J. E. *J. Am. Chem. Soc.* **1982**, *104*, 2157. (d) Luetkens, M. L., Jr.; Elcesser, W. L.; Huffman, J. C.; Sattelberger, A. P. *Inorg. Chem.* **1984**, *23*, 1718. (e) Venanzi, L. M. *Coord. Chem. Rev.* **1982**, *43*, 251.
(4) Hillhouse, G. L.; Bercaw, J. E. *Organometallics* **1982**, *1*, 1025.
(5) Gell, K. I.; Posin, B.; Schwartz, J.; Williams, G. M. *J. Am. Chem. Soc.* **1982**, *104*, 1846.
(6) Labinger, J. A.; Schwartz, J. *Angew. Chem., Int. Ed. Engl.* **1976**, *15*, 333.
(7) Jones, S. B.; Petersen, J. L. *Inorg. Chem.* **1981**, *20*, 2889.
(8) Wolczanski, P. T.; Bercaw, J. E. *Acc. Chem. Res.* **1980**, *13*, 121.
(9) Fryzuk, M. D.; Williams, H. D.; Rettig, S. J. *Inorg. Chem.* **1983**, *22*, 863.
(10) Fryzuk, M. D.; Carter, A.; Westerhaus, A. *Inorg. Chem.* **1985**, *24*, 642.
(11) (a) Pearson, R. G. *J. Chem. Educ.* **1968**, *45*, 581, 643. (b) Huheey, J. E. "Inorganic Chemistry", 3rd ed.; Harper and Row: New York, 1983; p 312.
(12) (a) Lappert, M. F.; Power, P.; Sanger, A. R.; Srivastava, R. C. "Metal and Metalloid Amides"; Wiley: Chichester, England, 1980; pp 472–477. (b) Andersen, R. A. *Inorg. Chem.* **1979**, *18*, 1724, 2928.

0020-1669/85/1324-4316$01.50/0

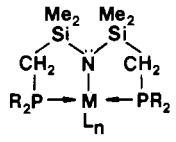

1

phosphine dissociation is reduced by virtue of the chelate effect.[13] Previous work from our laboratory exemplifies this strategy; bis(ligand) complexes[9] of the formula $MCl_2[N(SiMe_2CH_2PR_2)_2]_2$ (**2**: M = Zr, Hf; R = Me, Ph), and mono(ligand) derivatives[10] of the type $MCl_3[N(SiMe_2CH_2PR_2)_2]$ (**3**: M = Zr, Hf; R = Me, *i*-Pr, *t*-Bu) all show robust phosphine coordination even in the presence of added *hard* ligands such as amines or ethers.

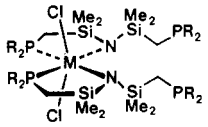

M	R
2a: Hf	Me
2b: Zr	Me
2c: Hf	Ph
2d: Zr	Ph

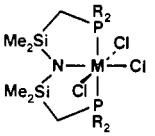

M	R
3a: Zr	Me
3b: Zr	*i*-Pr
3c: Zr	*t*-Bu
3d: Hf	Me
3e: Hf	*i*-Pr
3f: Hf	*t*-Bu

On the basis of the wealth of chemistry established for "later"-transition-metal complexes that contain ancillary phosphine ligands,[14] we anticipated that phosphine ligands bonded to the "early" transition metals[15] (i.e. Zr, Hf) should generate new types of reactivities. In particular, we are interested in the effects of this mixed donor ancillary ligand matrix on the chemistry of metal–hydrogen and metal–carbon bonds, since it is these latter types of reactive ligands that are involved in numerous organometallic transformations.

All of our attempts to substitute the metal–chloride bonds of the bis(ligand) derivatives **2** to generate the desired metal–hydride and/or metal–carbon bonds have been unsuccessful.[9] However, we have found that the mono(ligand) complexes **3** are very reactive and serve as convenient starting materials for the production of new organometallic derivatives.

In this full paper, we provide details on the synthesis, stability, and fluxional behavior of binuclear hafnium mixed-hydride–tetrahydroborate complexes of the general formula $[Hf[N(SiMe_2CH_2PMe_2)_2]]_2(\mu\text{-}H)_x(BH_4)_{6-x}$ (x = 2–4). Using the single-crystal X-ray structure of the x = 3 derivative, described herein, we have developed models to rationalize the unusual solution behavior of these binuclear hydrides of hafnium. What emerges from this investigation is a new type of intramolecular, intermetal BH_4^- migration process, which is undoubtedly a result of the stereochemistry at the metal center imposed by this new ancillary ligand system.

Experimental Section

General Information. All manipulations were performed under prepurified nitrogen in a Vacuum Atmospheres HE-553-2 glovebox equipped with a MO-40-2H Dri-Train or in standard Schlenk type glassware. $ZrCl_4$ (Aldrich) and $HfCl_4$ (Alfa) were sublimed prior to use. $LiBH_4$ (Alfa) was dried under vacuum; NMe_3 (Matheson) was dried over $LiAlH_4$ while PMe_3 (Strem) was used as received. $LiCH_2SiMe_3$ was prepared from $ClCH_2SiMe_3$ and Li metal in hexanes.[16] Solvents were dried, distilled, and degassed by standard procedures. Melting points were determined on a Mel-Temp apparatus in sealed capillaries under N_2 and are uncorrected. Carbon, hydrogen, nitrogen, and halogen analyses were performed by Peter Borda of this department. ^1H NMR spectra were recorded on one or more of the following instruments depending on the complexity of the particular spectrum: Bruker WP-80, Bruker WH-400 or Nicolet-Oxford 270 MHz. $^{31}P\{^1H\}$ and ^{11}B NMR spectra were run on the WP-80; all ^{31}P chemical shifts are referenced to external $P(OMe)_3$ set at +141.0 ppm relative to 85% H_3PO_4, while ^{11}B chemical shifts are referenced to external $B(OMe)_3$ set at −18.1 ppm relative to $BF_3{\cdot}Et_2O$. C_6D_6 and C_7D_8 were obtained from Aldrich, dried over activated 4-Å molecular sieves, and vacuum transferred prior to use. Infrared spectra were run on either a Pye-Unican SP-1100 or a Nicolet-5D-X spectrometer. The starting mono(ligand) derivatives $HfCl_3[N(SiMe_2CH_2PR_2)_2]$ (R = Me, *i*-Pr) were prepared by the literature procedures.[10]

$Hf(BH_4)_3[N(SiMe_2CH_2PMe_2)_2]$. To a solution of $HfCl_3[N(SiMe_2CH_2PMe_2)_2]$ (1.13 g, 2.00 mmol) in toluene (100 mL) was added solid $LiBH_4$ (~0.5 g, excess), and the mixture was stirred rapidly at 25 °C for 2 days. The mixture was filtered through Celite to give a clear, colorless solution, which was evaporated down to a volume of ~10 mL; after the addition of hexanes and cooling to −30 °C colorless crystals were obtained: yield 0.81 g (81%); mp 119 °C (dec); molecular weight (Signer, C_6D_6, 25 °C) 481 ± 20 (calcd 503.48). ^1H NMR (C_6D_6, ppm): PCH_3, 1.17 (virtual triplet, J_{app} = 4.0 Hz); PCH_2Si, 0.94 (virtual triplet, J_{app} = 6.0 Hz); $SiCH_3$, 0.31 (s); BH_4, ~2.9 (br q, $J_{^{11}B} \approx 88$ Hz). $^{31}P\{^1H\}$ NMR (C_6D_6, ppm): −20.03 (s). ^{11}B NMR (C_6D_6, ppm relative to external $B(OMe)_3$ at −18.1): −27.2 (br quin); low temperature spectra are broad and uninformative. IR (hexane, cm^{-1}): 2470, 2420 (ν(B–H^t)); 2110, 1950 (ν(B–H^b)); 1345 (δ(B–H)). Anal. Calcd for $C_{10}H_{40}B_3HfNP_2Si_2$: C, 24.93; H, 8.36; N, 2.90. Found: C, 24.60; H, 8.30; N, 2.77.

$Hf(BH_4)_3[N(SiMe_2CH_2P(i\text{-}Pr)_2)_2]$. To a solution of $HfCl_3[N(SiMe_2CH_2P(i\text{-}Pr)_2)_2]$ (0.50 g, 0.74 mmol) in toluene (50 mL) was added solid $LiBH_4$ (0.3 g, excess) and the suspension stirred rapidly for 1 day. The mixture was filtered through Celite and evaporated to dryness to give a white crystalline solid. Recrystallization from a minimum amount of toluene by the addition of hexanes gave large white crystals: yield 0.37 g (81%). ^1H NMR (C_6D_6, ppm): $PCH(CH_3)_2$, 1.95 (m); $PCH(CH_3)_2$, 1.95 (m); $PCH(CH_3)_2$, 1.02 (quint, $J_P = J_{CH}$ = 7.0 Hz); PCH_2Si (obscured); $SiCH_3$, 0.35 (s); BH_4, 3.5 (br lump). IR (KBr, cm^{-1}): 2530 (w), 2480 (s), 2410 (s), 2300 (w), 2240 (w), 2160 (m), 2110 (s), ~2000 (w), 1460 (s), 1340 (br, s), 1250 (s). $^{31}P\{^1H\}$ NMR (C_6D_6, ppm): 23.2 (s). Anal. Calcd for $C_{18}H_{56}B_3HfNP_2Si_2$: C, 35.11; H, 9.16; N, 2.27. Found: C, 35.33; H, 9.17; N, 2.36.

$[Hf[N(SiMe_2CH_2PMe_2)_2]]_2(\mu\text{-}H)_3(BH_4)_3$. PMe_3 (0.9 g, 11.8 mmol) was added to a solution of $Hf(BH_4)_3[N(SiMe_2CH_2PMe_2)_2]$ (0.93 g, 1.85 mmol) in toluene (25 mL) and the clear, colorless solution stirred for 2 days. The volatiles were removed under vacuum, the residue (contains H_3BPMe_3) was extracted with 2–3 mL of hexanes, and the extract was filtered through Celite and cooled to −30 °C for 12 h. Off-white crystals were obtained: yield 0.61 g (68%); mp 134–136 °C; molecular weight (Signer, C_6D_6, 25 °C) 980 ± 20 (calcd 965.46). ^1H NMR (C_7D_8, ppm): Hf–H–Hf, 8.68 (quintet, ^2J_P = 8.6 Hz); PCH_3, 1.37 (virtual triplet, J_{app} = 3.4 Hz); PCH_2Si, 0.94 (virtual triplet, J_{app} = 4.9 Hz); $SiCH_3$, 0.37 (s). $^{31}P\{^1H\}$ NMR (C_6D_6, ppm): −16.2 (s). ^{11}B NMR (C_6D_6, ppm): −49.2 (br quintet, $^1J_H \approx 95$ Hz). IR (hexanes, cm^{-1}): 2520 (w), 2425 (s), 2400 (w, sh), 2144 (s), 1545 (s) (B–H and Hf–H modes). Anal. Calcd for $C_{20}H_{71}B_3Hf_2N_2P_4Si_4$: C, 24.88; H, 7.41; N, 2.90; B, 3.36; P, 12.83. Found: C, 25.00; H, 7.08; N, 3.20; B, 3.69; P, 12.96. Boron and phosphorus analyses were carried out by Canadian MicroAnalytical Laboratory, Vancouver, Canada.

$[Hf[N(SiMe_2CH_2PMe_2)_2]]_2(\mu\text{-}H)_4(BH_4)_2$. To a solution of $Hf(BH_4)_3[N(SiMe_2CH_2PMe_2)_2]$ (1.30 g, 2.58 mmol) in toluene (50 mL) in a thick-walled flask (200 mL), equipped with a Teflon needle value, was condensed dry NMe_3 (~20 mL) and the solution stirred in the dark for 5–6 days. The volatiles were removed in vacuo (~4 h at 30–40 °C), and the residue was recrystallized from neat toluene by cooling to −30 °C to give yellow flakes: yield 0.62 g (51%); mp 146 °C. ^1H NMR (C_6D_6, ppm): Hf–*H*–Hf, 9.65 (quintet, J_P = 11.8 Hz); BH_4, ~2.0 (br lump); PCH_3, 1.48, 1.40 (virtual triplets, J_{app} = 3.4 Hz); PCH_2Si, 1.02 (br s); 0.81 (m); $SiCH_3$, 0.30, 0.24 (s). $^{31}P\{^1H\}$ NMR (C_6D_6, ppm): −11.4 (s). $^{31}P\{^1H\}$ NMR (C_7D_8, ppm, −40 °C): AB quartet, P_A −10.3, P_B −13.3 (J_{AB} = 46.4 Hz). IR (KBr, cm^{-1}): 2401 (s), 2376 (s), 2290 (m), 2225 (m), 2130 (s), 1411 (s), 1240 (vs) (B–H and Hf–H modes). Anal. Calcd for $C_{20}H_{68}B_2Hf_2N_2P_4Si_4$: C, 25.24; H, 7.20; N, 2.94. Found: C, 25.50; H, 7.20; N, 2.70.

$HfCl_2(CH_2SiMe_3)[N(SiMe_2CH_2PMe_2)_2]$. To a cold (−78 °C) solution of $HfCl_3[N(SiMe_2CH_2PMe_2)_2]$ (0.40 g, 0.70 mmol) in toluene (150 mL) was added $LiCH_2SiMe_3$ (66.5 mg, 0.69 mmol) in toluene (10 mL). The

(13) Cotton, F. A.; Wilkinson, G. "Advanced Inorganic Chemistry", 4th ed.; Wiley: New York, 1980; p 71.
(14) (a) Stelzer, O. *Top. Phosphorus Chem.* **1977**, *9*, 1. (b) MacAuliffe, C. A.; Levason, W. "Phosphine, Arsine and Stibene complexes of the Transition Elements"; Elsevier: Amsterdam, 1979. (c) Alyea, E.; Meek, D., Ed. "Catalytic Aspects of Metal Phosphine Complexes"; American Chemical Society: Washington, DC, 1982; *Adv. Chem. Ser.* No. 196.
(15) (a) Wengrovius, J. H.; Schrock, R. R. *J. Organomet. Chem.* **1981**, *205*, 319. (b) Choukroun, R.; Dahan, F.; Gervais, D. *J. Organomet. Chem.* **1984**, *266*, C33. (c) Wreford, S. S.; Whitney, J. F. *Inorg. Chem.* **1981**, *20*, 3918 and references therein.
(16) Prepared in a fashion identical with that described for $LiCH_2CMe_3$ in: Schrock, R. R.; Fellmann, J. D. *J. Am. Chem. Soc.* **1978**, *100*, 3359.

mixture was slowly allowed to warm to room temperature (~8 h), and then the toluene was removed, the residue extracted with hexanes (10–15 mL), and the extract filtered. Recrystallization from a minimum amount of hexanes at −30 °C generated yellow crystals: yield 0.27 g (61%). ^{1}H NMR (C_6D_6, ppm): PCH_3, 0.96 (filled-in doublet, $|^2J_P + {}^4J_P|$ = 9.0 Hz); $HfCH_2Si$, 0.55 (t, ^3J_P = 2.0 Hz); $CH_2Si(CH_3)_3$, 0.47 (s); $Si(CH_3)_2$, 0.20 (s). $^{31}P\{^1H\}$ NMR (C_6D_6, ppm): −22.8 (s). Anal. Calcd for $C_{14}H_{39}Cl_2HfNP_2Si_3$: C, 27.25; H, 6.37; N, 2.26. Found: C, 27.00; H, 6.25; N, 2.26.

$Hf(BH_4)_2CH_2SiMe_3[N(SiMe_2CH_2PMe_2)_2]$. To a solution of $HfCl_2(CH_2SiMe_3)[N(SiMe_2CH_2PMe_2)_2]$ (0.10 g, 0.16 mmol) in toluene (30 mL) was added solid $LiBH_4$ (0.1 g, excess) and the mixture stirred vigorously overnight. The mixture was filtered through Celite and pumped down to dryness. The residue was recrystallized from a minimum amount of hexanes at −30 °C to give the product as pale yellow crystals: yield 0.08 g (85%). ^{1}H NMR (C_6D_6, ppm): PCH_3, 1.03 (virtual triplet, J_{app} = 4 Hz); PCH_2Si, 0.78 (virtual triplet, J_{app} = 6 Hz); $CH_2Si(CH_3)_3$, 0.41 (s); $HfCH_2Si$, 0.29 (t, ^3J_P = 6.0 Hz); $Si(CH_3)_2$, 0.18 (s); BH_4, ~2.6 (broad lump). $^{31}P\{^1H\}$ NMR (C_6D_6, ppm): −18.1 (s). Anal. Calcd for $C_{14}H_{47}B_2HfNP_2Si_3$: C, 29.20; H, 8.22; N, 2.43. Found: C, 29.12; H, 8.13; N, 2.40.

$[HfCl_2[N(SiMe_2CH_2PMe_2)_2]]_2(\mu\text{-}H)_2$. A solution of $HfCl_2(CH_2SiMe_3)[N(SiMe_2CH_2PMe_2)_2]$ (0.20 g, 0.33 mmol) in toluene (30 mL) in a 100-mL thick-walled reactor fitted with a Kontes needle valve was cooled to −196 °C and H_2 admitted to a pressure of 1 atm. The reactor was sealed and the solution allowed to warm to room temperature and then stirred vigorously for 18 h. After removal of the H_2 and the toluene, the residue was recrystallized from a minimum amount of toluene by the addition of hexanes and cooling to −30 °C: yield 0.13 g (75%). ^{1}H NMR (C_6D_6, ppm): Hf–H–Hf, 13.52 (quintet, ^2J_P = 10.0 Hz); PCH_3, 1.37 (virtual triplet, J_{app} = 3.5 Hz); PCH_2Si, 1.07 (virtual triplet, J_{app} = 6.5 Hz); $SiCH_3$, 0.44 (s). $^{31}P\{^1H\}$ NMR (C_6D_6, ppm): −12.3 (s). Anal. Calcd for $C_{10}H_{29}Cl_2HfNP_2Si_2$: C, 22.62; H, 5.50; N, 2.63; Cl, 13.35. Found: C, 22.69; H, 5.63; N, 2.50; Cl, 13.14. IR (KBr, cm^{-1}): 1420 (s, br), 1250 (s).

Attempted Preparation of $[Hf[N(SiMe_2CH_2PMe_2)_2]]_2(\mu\text{-}H)_2(BH_4)_4$. Method 1. To a solution of $[HfCl_2[N(SiMe_2CH_2PMe_2)_2]]_2(\mu\text{-}H)_2$ (0.10 g, 0.094 mmol) in toluene (30 mL) was added $LiBH_4$ (~0.1 g, excess) and the mixture stirred rapidly for 12 h. The mixture was filtered through Celite and pumped to dryness in vacuo. The crude residue was analyzed by ^{1}H NMR and $^{31}P\{^1H\}$ NMR to be an equimolar mixture of $[Hf[N(SiMe_2CH_2PMe_2)_2]]_2(\mu\text{-}H)_3(BH_4)_3$ and $Hf(BH_4)_3[N(SiMe_2CH_2PMe_2)_2]$.

Method 2. A solution of $Hf(BH_4)_2CH_2SiMe_3[N(SiMe_2CH_2PMe_2)_2]$ (0.12 g, 0.21 mmol) in toluene (10 mL) was pressurized to ~4 atm of H_2 as described above for the preparation of $[HfCl_2[N(SiMe_2CH_2PMe_2)_2]]_2(\mu\text{-}H)_2$ and stirred for 12 h. After removal of the toluene in vacuo, NMR analysis of the crude mixture gave results identical with those found in method 1.

Deuteration of $Hf(BH_4)_2CH_2SiMe_3[N(SiMe_2CH_2PMe_2)_2]$. The identical procedure described for method 2, immediately above, was followed except that D_2 was used instead of H_2.

^{31}P NMR Tube Reactions. A number of the above transformations are conventiently followed by $^{31}P\{^1H\}$ NMR. The following example exemplifies this procedure. A solution of $Hf(BH_4)_3[N(SiMe_2CH_2PMe_2)_2]$ (0.12 g, 0.24 mmol) was dissolved in C_6D_6 (2.5 mL) and placed in a 10 mm NMR tube attached to a joint which in turn could be attached to a vacuum line via a Kontes needle valve; NMe_3 (0.42 g, 30 equiv) was vacuum transferred from $LiAlH_4$ into the NMR tube and the tube sealed with a torch. Periodic monitoring by $^{31}P\{^1H\}$ was then carried out with use of the ^{31}P chemical shifts described above.

X-ray Crystallographic Analysis of $[Hf[N(SiMe_2CH_2PMe_2)_2]]_2(\mu\text{-}H)_3(BH_4)_3$. Crystallographic data are presented in Table I. The crystal was sealed under nitrogen in a Lindemann glass capillary and mounted in a general orientation. The use of an unusually large crystal for data collection was necessitated by the poor quality of the smaller specimens examined and by the difficulty of handling this material. The unit-cell parameters were refined by least squares on $2(\sin\theta)/\lambda$ values for 25 reflections with 2θ = 50–53°. The intensities of the reflections (−9,7,0), 1,−13,1), and (−1,−8,6) (monitored 1 h of X-ray exposure time) decreased by 6, 14, and 10%, respectively, during the data collection. A correction for nonuniform decay[17] was applied during the data processing.[18] The data were corrected for absorption (Gaussian integration, 302 sampling points).[19,20] Corrections for the presence of extinction were not applicable.

Table I. Crystallographic Data[a]

compd	$Hf_2[N(SiMe_2CH_2PMe_2)_2]H_3(BH_4)_3$
formula	$C_{20}H_{71}B_3Hf_2N_2P_4Si_4$
fw	965.44
cryst syst	triclinic
space group	$P\bar{1}$
a, Å	13.333 (3)
b, Å	18.722 (3)
c, Å	9.690 (3)
α, deg	94.02 (2)
β, deg	107.04 (2)
γ, deg	109.14 (2)
V, Å^3	2147
Z	2
D_{calcd}, g/cm^3	1.493
$F(000)$	960
μ(Mo Kα), cm^{-1}	50.6
cryst dimens, mm	0.25 × 0.36 × 0.63 [6 faces: ±(0,1,0), (1,0,0), (−3,2,0), ±(2,1,−3)]
transmission factors	0.146–0.320
scan type	ω–2θ
scan range (in ω), deg	0.70 + 0.35 tan θ
scan speed, deg/min	1.68–10.06
data collected	$\pm h,\pm k,\pm l$
$2\theta_{max}$, deg	55
unique reflcns	9827
reflcns with $I \geq 3\sigma(I)$	7675
no. of variables	328
R	0.042
R_w	0.057
S	2.481
mean Δ/σ (final cycle)	0.05
max Δ/σ (final cycle)	0.41
residual density, e/Å^3	4.1 (near Hf)

[a] Further information: temperature 22 °C, Enraf-Nonius CAD4-F diffractometer, Mo Kα radiation ($\lambda_{K\alpha_1}$ = 0.709 Å, $\lambda_{K\alpha_2}$ = 0.713 59 Å), graphite monochromator, takeoff angle 2.7°, aperture (2.00 + tan θ) × 4.0 mm at a distance of 173 mm from the crystal, scan range extended by 25° on both sides for background measurement, $\sigma^2(I) = S + 2B + [0.04(S - B)]^2$ (S = scan count, B = normalized background count), function minimized $\sum w(|F_o| - |F_c|)^2$, where $w = 1/\sigma^2(F)$, $R = \sum||F_o| - |F_c||/\sum|F_o|$, $R_w = (\sum w(|F_o| - |F_c|)^2/\sum w|F_o|^2)^{1/2}$, $S = (\sum w(|F_o| - |F_c|)^2/(m - n))^{1/2}$. Values given for R, R_w, and S are based on those reflections with $I \geq 3\sigma(I)$. No equivalent reflections were collected; none were multiply measured.

The centrosymmetric space group $P\bar{1}$ was indicated by both the E statistics and the Patterson function, from which the Hf, P, and Si coordinates were determined. The remaining non-hydrogen atoms were positioned from a subsequent difference map, and refinement of all non-hydrogen atoms with anisotropic thermal parameters resulted in R = 0.047 and R_w = 0.075. A difference map at this point clearly revealed the positions of all 71 hydrogen atoms (Fourier grid size 0.33 Å). Attempts to refine the 15 metal and borohydride H atoms (the remaining H atoms being fixed in idealized positions on the basis of the observed positions with C–H = 0.98 Å) were only partially successful. All four protons associated with B(1) were refined to reasonable positions. It is clear that the $H_4B(1)$ group is tridentate, both from the Hf···B(1) distance of 2.322 (8) Å and from the refined H positions.[33] For the $H_4B(2)$ group, three H atoms were refined successfully (all but H(B2c)). The Hf···B(2) distance of 2.583 (6) Å and the locations of the refined H positions are consistent with an unsymmetrical bidentate mode of coordination. In the case of B(3), two H atoms (H(B3b) and H(B3c)) were refined to good positions and a third (H(B3d)) to a marginally acceptable position. There remains some ambiguity regarding the coordination mode of the $H_4B(3)$ ligand. The Hf···B(3) distance is 2.636 (7) Å, 0.053 (9) Å longer than Hf···B(2). If the refined H(B3b) and H(B3c) positions are in error, it is possible that the $H_4B(3)$ ligand is bidentate. If the H(B3b) position is assumed to be accurate, the Hf–H(B36b) distance of 1.93 Å is essentially the same as the mean Hf–H(metal hydride) distance of 1.90 (8) Å while the Hf···H(B3a) distance would be calculated to be

(17) Ibers, J. A. *Acta Crystallogr., Sect. B: Struct. Crystallogr. Cryst. Chem.* **1969**, *B25*, 1667–1668.

(18) The computer programs used include locally written programs for data processing and locally modified versions of the following: ORFLS, full-matrix least squares, and ORFFE, function and errors, by W. R. Busing, K. O. Martin, and H. J. A. Levy; FORDAP, Patterson and Fourier syntheses, by A. Zalkin; ORTEP II, illustrations, by C. K. Johnson.

(19) Coppens, P.; Leiserowitz, L.; Rabinovich, D. *Acta Crystallogr.* **1965**, *18*, 1035–1038.

(20) Busing, W. R.; Levy, H. A. *Acta Crystallogr.* **1967**, *22*, 457–464.

Table II. Final Positional (Fractional ×10⁴; Hf, P, and Si ×10⁵; H ×10³) and Isotropic Thermal Parameters ($U \times 10^3$ Å²) with Estimated Standard Deviations in Parentheses

atom	x	y	z	U_{eq}/U_{iso}[a]
Hf(1)	53993 (2)	24967 (1)	58944 (2)	37
Hf(2)	28155 (2)	21975 (1)	50902 (2)	40
P(1)	61559 (14)	36763 (10)	45353 (17)	46
P(2)	57476 (15)	17709 (11)	82221 (21)	55
P(3)	23514 (15)	11216 (10)	27080 (19)	54
P(4)	24189 (14)	30556 (10)	71979 (18)	47
Si(1)	67783 (14)	43502 (10)	76711 (18)	48
Si(2)	77835 (15)	32301 (12)	89323 (20)	53
Si(3)	2201 (16)	14176 (12)	23533 (21)	58
Si(4)	1039 (15)	20060 (12)	51179 (23)	57
N(1)	6726 (4)l	3408 (3)	7627 (5)	43
N(2)	920 (4)	1847 (3)	4143 (5)	45
C(1)	6137 (5)	4449 (4)	5697 (7)	68
C(2)	7266 (6)	2148 (5)	8948 (9)	69
C(3)	850 (6)	686 (5)	1994 (9)	72
C(4)	996 (6)	2469 (5)	7069 (8)	67
C(5)	7623 (6)	3944 (5)	4661 (9)	66
C(6)	5448 (7)	3718 (5)	2633 (7)	68
C(7)	5282 (7)	2047 (6)	9702 (9)	73
C(8)	5282 (8)	714 (5)	8022 (13)	97
C(9)	2844 (9)	1470 (6)	1229 (10)	96
C(10)	2869 (7)	346 (4)	2986 (10)	75
C(11)	2370 (8)	3997 (4)	6973 (9)	73
C(12)	3224 (7)	3209 (5)	9131 (8)	68
C(13)	5977 (8)	4596 (5)	8775 (9)	78
C(14)	8242 (7)	5095 (5)	8388 (10)	83
C(15)	8170 (8)	3772 (6)	10840 (8)	87
C(16)	9094 (6)	3435 (6)	8449 (10)	74
C(17)	323 (8)	2083 (6)	993 (9)	86
C(18)	−1339 (6)	858 (5)	1793 (10)	78
C(19)	−686 (8)	2643 (6)	4294 (13)	100
C(20)	−975 (8)	1137 (6)	5372 (12)	99
B(1)	5994 (8)	1711 (6)	4621 (12)	73
B(2)	2796 (6)	3332 (4)	3726 (8)	45
B(3)	2336 (6)	1127 (4)	6674 (8)	50
H(1)	387 (6)	183 (4)	568 (8)	59 (21)
H(2)	428 (5)	279 (3)	646 (7)	57 (16)
H(3)	409 (5)	253 (3)	443 (7)	54 (17)
H(B1a)	686	225	554	73
H(B1b)	539	201	372	73
H(B1c)	540	129	530	73
H(B1d)	630	132	391	85
H(B2a)	336	333	505	45
H(B2b)	236	264	298	45
H(B2c)	205	357	372	58
H(B2d)	341	374	317	58
H(B3a)	203	86	530	51
H(B3b)	263	186	687	51
H(B3c)	156	85	712	63
H(B3d)	313	96	734	63

[a] $U_{eq} = {}^1/_3$[trace U_{diag}].

2.43 Å with an assumed B–H distance of 1.29 Å. This 2.43-Å distance is about 0.2 Å longer than any associated with the bidentate $H_4B(2)$ ligand in the present case and about 0.3 Å longer than the maximum Hf–H(bidentate BH_4) distance in the neutron diffraction structure of $(\eta^5\text{-}C_5H_4CH_3)_2Hf(BH_4)_2$.[34] The $H_4B(3)$ ligand may be considered monodentate on these grounds. A neutron diffraction study of the structure would be required to unambiguously determine the coordination mode of the $H_4B(3)$ ligand. The BH_4 hydrogen positions were then idealized from the observed positions with B–H (bridging, including H(B3a)) = 1.29 Å and B–H (terminal) = 1.21 Å and included as fixed contributors to the structure. The three bridging metal hydride atoms were refined with isotropic thermal parameters.

Neutral-atom scattering factors and anomalous scattering terms (Hf, P, Si) were taken from ref 21. The final statistics appear in Table I. Final atomic coordinates and isotropic thermal parameters, bond distances, bond angles, and intraannular torsion angles are given in Tables II–V, respectively. Calculated coordinates and isotropic thermal parameters for the "organic" hydrogen atoms, anisotropic thermal parameters, torsion angles, and measured and calculated structure factor amplitudes

(21) "International tables for X-ray Crystallography"; Kynoch Press: Birmingham, England, 1974; Vol. IV.

Table III. Bond Lengths (Å) with Estimated Standard Deviations in Parentheses

Hf(1)–P(1)	2.712 (2)	P(2)–C(8)	1.847 (9)
Hf(1)–P(2)	2.717 (2)	P(3)–C(3)	1.786 (8)
Hf(1)–N(1)	2.176 (5)	P(3)–C(9)	1.820 (9)
Hf(1)–H(1)	1.95 (7)	P(3)–C(10)	1.805 (8)
Hf(1)–H(2)	1.95 (6)	P(4)–C(4)	1.815 (8)
Hf(1)–H(3)	1.93 (6)	P(4)–C(11)	1.811 (7)
Hf(1)–H(B1a)	2.25	P(4)–C(12)	1.813 (7)
Hf(1)–H(B1b)	2.23	Si(1)–N(1)	1.740 (5)
Hf(1)–H(B1c)	2.29	Si(1)–C(1)	1.902 (6)
Hf(2)–P(3)	2.732 (2)	Si(1)–C(13)	1.850 (8)
Hf(2)–P(4)	2.786 (2)	Si(1)–C(14)	1.876 (8)
Hf(2)–N(2)	2.264 (5)	Si(2)–N(1)	1.738 (5)
Hf(2)–H(1)	1.73 (7)	Si(2)–C(2)	1.917 (8)
Hf(2)–H(2)	1.91 (6)	Si(2)–C(15)	1.883 (9)
Hf(2)–H(3)	1.91 (6)	Si(2)–C(16)	1.867 (8)
Hf(2)–H(B2a)	2.01	Si(3)–N(2)	1.700 (5)
Hf(2)–H(B2b)	2.25	Si(3)–C(3)	1.886 (8)
Hf(2)–H(B3a)	2.43	Si(3)–C(17)	1.879 (9)
Hf(2)–H(B3b)	1.93	Si(3)–C(18)	1.882 (8)
P(1)–C(1)	1.781 (7)	Si(4)–N(2)	1.715 (5)
P(1)–C(5)	1.817 (7)	Si(4)–C(4)	1.876 (8)
P(1)–C(6)	1.828 (7)	Si(4)–C(19)	1.906 (9)
P(2)–C(2)	1.803 (7)	Si(4)–C(20)	1.872 (9)
P(2)–C(7)	1.827 (8)		

(Tables VI–IX) and a stereoview of the refined BH_4 protons are available as supplementary material.[22]

Results and Discussion

Synthesis and Structure of Mixed-Hydride–Tetrahydroborate Complexes. The starting material for the preparation of the binuclear mixed-hydride–tetrahydroborate derivatives is the mononuclear tris(tetrahydroborate) complex $Hf(BH_4)_3[N(SiMe_2CH_2PMe_2)_2]$ (**4**), which is prepared from the mono(ligand) precursor **3d** and excess $LiBH_4$ in toluene. This reaction can be extended[23] to the mono(ligand) derivative of hafnium containing bulky isopropyl substituents (**3e**) as summarized in eq 1. The

$$\underset{\substack{\textbf{3d},\ R = Me\\ \textbf{3e},\ R = i\text{-}Pr}}{HfCl_3[N(SiMe_2CH_2PR_2)_2]} + 3LiBH_4 \xrightarrow[(-3LiCl)]{\text{toluene}} \underset{\substack{\textbf{4},\ R = Me\\ \textbf{5},\ R = i\text{-}Pr}}{Hf(BH_4)_3[N(SiMe_2CH_2PR_2)_2]} \quad (1)$$

reaction of excess $LiBH_4$ with the mono(ligand) precursors containing *tert*-butyl substituents (**3c,f**) proceeds very slowly to give a mixture of products that we have not fully characterized.

The tris(tetrahydroborate) complexes **4** and **5** have similar structures on the basis of IR and NMR data. They are mononuclear in solution, with the mixed-donor ligand bound in a tridentate fashion; this is evidenced by both the downfield shift of ^{31}P resonances (compared to those of the free ligand) due to coordination and the presence of virtual triplets in the ^1H NMR spectra for the methylene (PCH_2Si) resonances. The BH_4^- units bind in a bidentate mode by comparison of the infrared spectra of complexes **4** and **5** to those of known systems;[24] in particular, the strong doublet in the terminal B–H stretching frequency region (2400–2600 cm^{-1}) is diagnostic of this type of coordination. The broad resonance in the ^1H NMR spectrum due to the BH_4^- ligands indicates rapid exchange of terminal and bridging B–H bonds on the ^1H NMR time scale; the single, broad quintet observed in the ^{11}B NMR spectrum is consistent with this observation.[24]

The structure of these tris(tetrahydroborate) complexes is not obvious in the absence of crystallographic information. In solution, the ^1H NMR spectrum is compatible with the tridentate ligand

(22) See paragraph at end of paper regarding details of supplementary material available.

(23) The zirconium derivatives $Zr(BH_4)_3[N(SiMe_2CH_2PR_2)_2]$ (R = Me, *i*-Pr) are also accessible by this procedure (Westerhaus, A., unpublished results).

(24) Marks, T. J.; Kolb, J. R. *Chem. Rev.* **1977**, *77*, 263.

Scheme I

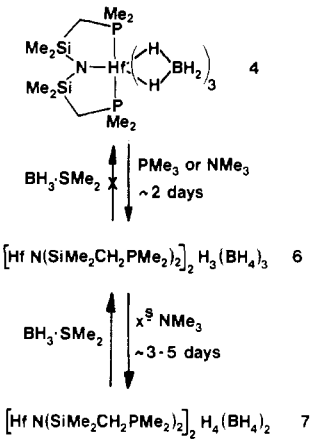

coordinated in a meridional fashion with the trans-disposed (vide infra) phosphine donors giving rise to the virtual triplet patterns.[25] However, by symmetry this requires that the three bidentate BH_4^- ligands reside in two nonequivalent sites: one BH_4^- being trans to the amide donor while the remaining two are cis to the amide ligand (assuming a basic octahedral geometry). Since we observe only one environment for the BH_4^- ligands in the ^{11}B NMR spectrum, there must be rapid exchange between the two proposed sites. Attempts to freeze out this process[26] on both the ^1H and ^{11}B NMR time scales have not been successful.

In certain cases, transition-metal tetrahydroborate complexes serve as precursors to metal hydride derivatives if BH_3 can be cleaved from the BH_4^- unit;[27] typically, strong σ donors such as tertiary amines or phosphines are effective in this regard. If PMe_3 (6–8 equiv) is added to a toluene solution of $Hf(BH_4)_3[N(SiMe_2CH_2PMe_2)_2]$ (**4**), a binuclear mixed-hydride–tetrahydroborate complex (**6**), with the molecular formula $Hf_2[N(SiMe_2CH_2PMe_2)_2]_2(H)_3(BH_4)_3$, can be isolated after 2 days in ~65% yield by fractional crystallization;[28] by ^1H and ^{31}P NMR this reaction (eq 2) appears to be quantitative. NMe_3 and NEt_3

$$\underset{\mathbf{4}}{Hf(BH_4)_3[N(SiMe_2CH_2PMe_2)_2]} \xrightarrow[(-H_3B{<}PMe_3)]{PMe_3} \underset{\mathbf{6}}{Hf_2[N(SiMe_2CH_2PMe_2)_2]_2(H)_3(BH_4)_3} \quad (2)$$

also generate **6** under similar conditions as evidenced by $^{31}P\{^1H\}$ NMR (vide infra); however, use of the latter amine complicates isolation since the borane adduct, H_3BNEt_3, is not volatile and has a solubility similar to that of **6**. Less basic amines, such as pyridine, and ethers, such as tetrahydrofuran, do not cleave BH_3 from **4d**, suggesting that a minimum basicity is required for this transformation.

Monitoring the conversion of **4** to **6** by $^{31}P\{^1H\}$ NMR using 6–8 equiv of NMe_3 indicates that **6** forms at the expense of **4** without any observable intermediates. Although we initially reported[28] that further reaction of **6** with NMe_3 does not occur, we have since found that in the presence of a huge excess of NMe_3 (>100 equiv) another mixed-hydride–tetrahydroborate derivative is formed after 5 days (eq 3).

$$\underset{\mathbf{4}}{Hf(BH_4)_3[N(SiMe_2CH_2PMe_2)_2]} \xrightarrow[5\ \text{days}]{\text{excess } NMe_3} \underset{\mathbf{7}}{Hf_2[N(SiMe_2CH_2PMe_2)_2]_2(H)_4(BH_4)_2} \quad (3)$$

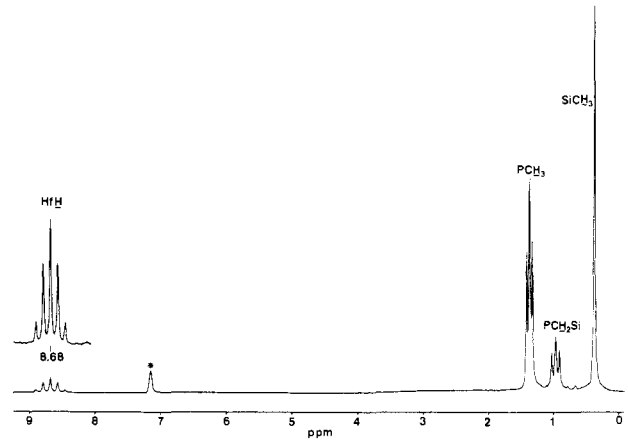

Figure 1. 80-MHz ^1H NMR spectrum (C_6D_6) of the binuclear trihydride $[Hf[N(SiMe_2CH_2PMe_2)_2]]_2(\mu\text{-}H)_3(BH_4)_3$ (**6**).

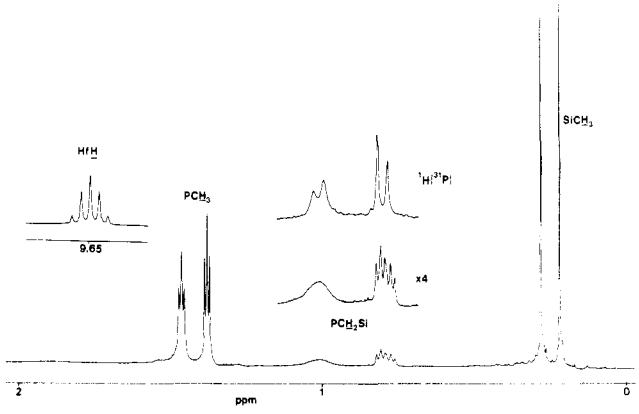

Figure 2. 400-MHz ^1H NMR spectrum (C_6D_6) of the binuclear tetrahydride $[Hf(N(SiMe_2CH_2PMe_2)_2]]_2(\mu\text{-}H)_4(BH_4)_2$. A portion of the $^1H\{^{31}P\}$ spectrum is also shown.

Again, monitoring the reaction of ~30 equiv of NMe_3 with **4** by $^{31}P\{^1H\}$ NMR shows initial formation of **6** (over a period of 1 day), which then is slowly transformed into **7** (over a period of 1 week); other minor peaks are observed in the $^{31}P\{^1H\}$ NMR spectrum, but they appear to be side products and have not been characterized. This experiment suggests that the trihydride–tris(tetrahydroborate) complex **6** is an intermediate in the formation of the tetrahydride–bis(tetrahydroborate) derivative **7**; in fact, this latter complex can be converted back to **6** by addition of 1 equiv of $BH_3{\cdot}SMe_2$ as outlined in Scheme I. Interestingly, the addition of excess $BH_3{\cdot}SMe_2$ does not appear to regenerate the starting tris(tetrahydroborate) complex **4**; rather, other hydride complexes are formed that have so far eluded characterization.[29]

Solution spectroscopic analysis of both of the binuclear mixed-hydride–tetrahydroborate complexes **6** and **7** provides a certain amount of information on gross structural features. That both complexes are binuclear with multiple bridging hydrides[30] is apparent from the ^1H NMR spectra (Figures 1 and 2), wherein the hydride ligands appear as a binomial *quintet* at 8.68 ppm for **6**, and at 9.65 ppm for **7**, due to coupling with *four* magnetically equivalent phosphorus nuclei; a solution molecular weight determination for **6** confirms this proposal. Accurate integration of the hydride resonance of **6** in the ^1H NMR spectrum indicates that there are *three* bridging hydrides per dimer. More conclusive evidence is obtained from the ^{31}P NMR spectrum of **6**: with

(25) (a) Assignment of a meridional stereochemistry based simply on the observation of a virtual triplet pattern is fraught with uncertainty;[10,25b] however, a facial geometry can be excluded because of the observed singlet for the silylmethyl protons and the simplicity of the methylene (PCH_2Si) resonance. (b) Ogilvie, F. B.; Jenkins, J. M.; Verkade, J. G. *J. Am. Chem. Soc.* **1970**, *92*, 1916.

(26) This type of process does not appear to have been observed previously.[24]

(27) James, B. C.; Narda, R. K.; Wallbridge, M. G. H. *Inorg. Chem.* **1967**, *6*, 1979.

(28) A portion of this work has been described in preliminary form in: Fryzuk, M. D.; Williams, H. D. *Organometallics* **1983**, *2*, 162.

(29) In the presence of excess $BH_3{\cdot}SMe_2$ it appears that one or two of the phosphine ligands dissociates from Hf and binds BH_3, on the basis of $^{31}P\{^1H\}$ NMR.

(30) Other binuclear metal systems with multiply bridging hydrides are known. $[ReH_2(PEt_2Ph)_2]_2(\mu\text{-}H)_4$ and $[Ir(\eta^5\text{-}C_5Me_5)]_2(\mu\text{-}H)_3^+$: Bau, R.; Carroll, W. E.; Hart, D. W.; Teller, R. G.; Koetzle, T. F. In ref 3a, p 73. $[IrH(dppp)]_2(\mu\text{-}H)_3^+$: Wang, H. H.; Pignolet, L. H. *Inorg. Chem.* **1980**, *19*, 1470. $[TaCl_2(PMe_3)_2]_2(\mu\text{-}H)_2$: Wilson, R. B., Jr.; Sattelberger, A. P.; Huffman, J. C. *J. Am. Chem. Soc.* **1982**, *104*, 858.

Table IV. Bond Angles (deg) with Estimated Standard Deviations in Parentheses

P(1)–Hf(1)–P(2)	149.57 (5)	H(3)–Hf(2)–H(B2a)	67
P(1)–Hf(1)–N(1)	74.49 (13)	H(3)–Hf(2)–H(B2b)	70
P(1)–Hf(1)–H(1)	131 (2)	H(3)–Hf(2)–H(B3a)	119
P(1)–Hf(1)–H(2)	100 (2)	H(3)–Hf(2)–H(B3b)	133
P(1)–Hf(1)–H(3)	74 (2)	H(B2a)–Hf(2)–H(B2b)	59
P(1)–Hf(1)–H(B1a)	80	H(B2a)–Hf(2)–H(B3a)	173
P(1)–Hf(1)–H(B1b)	71	H(B2a)–Hf(2)–H(B3b)	119
P(1)–Hf(1)–H(B1c)	123	H(B2b)–Hf(2)–H(B3a)	123
P(2)–Hf(1)–N(1)	77.18 (14)	H(B2b)–Hf(2)–H(B3b)	156
P(2)–Hf(1)–H(1)	78 (2)	H(B3a)–Hf(2)–H(B3b)	56
P(2)–Hf(1)–H(2)	91 (2)	Hf(1)–P(1)–C(1)	100.0 (2)
P(2)–Hf(1)–H(3)	135 (2)	Hf(1)–P(1)–C(5)	115.0 (3)
P(2)–Hf(1)–H(B1a)	85	Hf(1)–P(1)–C(6)	124.1 (3)
P(2)–Hf(1)–H(B1b)	122	C(1)–P(1)–C(5)	104.4 (4)
P(2)–Hf(1)–H(B1c)	67	C(1)–P(1)–C(6)	108.1 (3)
N(1)–Hf(1)–H(1)	134 (2)	C(5)–P(1)–C(6)	103.4 (4)
N(1)–Hf(1)–H(2)	89 (2)	Hf(1)–P(2)–C(2)	100.4 (2)
N(1)–Hf(1)–H(3)	130 (2)	Hf(1)–P(2)–C(7)	115.8 (3)
N(1)–Hf(1)–H(B1a)	83	Hf(1)–P(2)–C(8)	122.8 (4)
N(1)–Hf(1)–H(B1b)	130	C(2)–P(2)–C(7)	105.9 (4)
N(1)–Hf(1)–H(B1c)	125	C(2)–P(2)–C(8)	107.2 (4)
H(1)–Hf(1)–H(2)	53 (3)	C(7)–P(2)–C(8)	103.4 (5)
H(1)–Hf(1)–H(3)	57 (3)	Hf(2)–P(3)–C(3)	105.2 (3)
H(1)–Hf(1)–H(B1a)	133	Hf(2)–P(3)–C(9)	116.8 (3)
H(1)–Hf(1)–H(B1b)	96	Hf(2)–P(3)–C(10)	118.5 (3)
H(1)–Hf(1)–H(B1c)	77	C(3)–P(3)–C(9)	108.1 (4)
H(2)–Hf(1)–H(3)	59 (2)	C(3)–P(3)–C(10)	106.4 (4)
H(2)–Hf(1)–H(B1a)	172	C(9)–P(3)–C(10)	101.1 (4)
H(2)–Hf(1)–H(B1b)	131	Hf(2)–P(4)–C(4)	102.3 (2)
H(2)–Hf(1)–H(B1c)	129	Hf(2)–P(4)–C(11)	120.2 (3)
H(3)–Hf(1)–H(B1a)	128	Hf(2)–P(4)–C(12)	121.0 (3)
H(3)–Hf(1)–H(B1b)	73	C(4)–P(4)–C(11)	104.7 (4)
H(3)–Hf(1)–H(B1c)	105	C(4)–P(4)–C(12)	103.9 (4)
H(B1a)–Hf(1)–H(B1b)	56	C(11)–P(4)–C(12)	102.5 (4)
H(B1a)–Hf(1)–H(B1c)	55	N(1)–Si(1)–C(1)	106.9 (3)
H(B1b)–Hf(1)–H(B1c)	56	N(1)–Si(1)–C(13)	112.8 (3)
P(3)–Hf(2)–P(4)	158.59 (5)	N(1)–Si(1)–C(14)	114.2 (3)
P(3)–Hf(2)–N(2)	79.85 (13)	C(1)–Si(1)–C(13)	108.9 (3)
P(3)–Hf(2)–H(1)	78 (2)	C(1)–Si(1)–C(14)	106.6 (4)
P(3)–Hf(2)–H(2)	126 (2)	C(13)–Si(1)–C(14)	107.2 (4)
P(3)–Hf(2)–H(3)	74 (2)	N(1)–Si(2)–C(2)	107.7 (3)
P(3)–Hf(2)–H(B2a)	122	N(1)–Si(2)–C(15)	113.6 (3)
P(3)–Hf(2)–H(B2b)	68	N(1)–Si(2)–C(16)	112.8 (3)
P(3)–Hf(2)–H(B3a)	63	C(2)–Si(2)–C(15)	109.1 (4)
P(3)–Hf(2)–H(B3b)	119	C(2)–Si(2)–C(16)	104.8 (4)
P(4)–Hf(2)–N(2)	79.10 (13)	C(15)–Si(2)–C(16)	108.5 (4)
P(4)–Hf(2)–H(1)	118 (2)	N(2)–Si(3)–C(3)	105.7 (3)
P(4)–Hf(2)–H(2)	75 (2)	N(2)–Si(3)–C(17)	115.2 (4)
P(4)–Hf(2)–H(3)	126 (2)	N(2)–Si(3)–C(18)	117.8 (3)
P(4)–Hf(2)–H(B2a)	67	C(3)–Si(3)–C(17)	109.3 (4)
P(4)–Hf(2)–H(B2b)	108	C(3)–Si(3)–C(18)	105.1 (4)
P(4)–Hf(2)–H(B3a)	107	C(17)–Si(3)–C(18)	103.2 (4)
P(4)–Hf(2)–H(B3b)	56	N(2)–Si(4)–C(4)	110.4 (3)
N(2)–Hf(2)–H(1)	143 (2)	N(2)–Si(4)–C(19)	112.5 (4)
N(2)–Hf(2)–H(2)	154 (2)	N(2)–Si(4)–C(20)	116.9 (4)
N(2)–Hf(2)–H(3)	138 (2)	C(4)–Si(4)–C(19)	108.6 (4)
N(2)–Hf(2)–H(B2a)	102	C(4)–Si(4)–C(20)	101.5 (4)
N(2)–Hf(2)–H(B2b)	70	C(19)–Si(4)–C(20)	106.1 (5)
N(2)–Hf(2)–H(B3a)	74	Hf(1)–N(1)–Si(1)	119.6 (2)
N(2)–Hf(2)–H(B3b)	88	Hf(1)–N(1)–Si(2)	121.8 (3)
H(1)–Hf(2)–H(2)	57 (3)	Si(1)–N(1)–Si(2)	118.5 (3)
H(1)–Hf(2)–H(3)	61 (3)	Hf(2)–N(2)–Si(3)	120.3 (3)
H(1)–Hf(2)–H(B2a)	115	Hf(2)–N(2)–Si(4)	124.0 (3)
H(1)–Hf(2)–H(B2b)	126	Si(3)–N(2)–Si(4)	115.7 (3)
H(1)–Hf(2)–H(B3a)	69	P(1)–C(1)–Si(1)	107.3 (3)
H(1)–Hf(2)–H(B3b)	77	P(2)–C(2)–Si(2)	108.2 (3)
H(2)–Hf(2)–H(3)	60 (2)	P(3)–C(3)–Si(3)	109.4 (4)
H(2)–Hf(2)–H(B2a)	65	P(4)–C(4)–Si(4)	111.2 (4)
H(2)–Hf(2)–H(B2b)	115	Hf(1)–H(1)–Hf(2)	117 (4)
H(2)–Hf(2)–H(B3a)	116	Hf(1)–H(2)–Hf(2)	109 (3)
H(2)–Hf(2)–H(B3b)	80	Hf(1)–H(3)–Hf(2)	110 (3)

broad-band proton decoupling, a singlet is found; however, when the ligand protons ($P(CH_3)_2$, PCH_2Si) are selectively decoupled, a *quartet* is observed due to coupling with the three bridging hydrides. A similar selective decoupling experiment for **7** produces a *quintet* in the ^{31}P NMR, indicating that there are *four* bridging hydrides on this complex. The BH_4^- resonances of **6** and **7** in the ^1H NMR spectrum are broad and uninformative. The IR spectrum of **6** shows a number of bands in the B–H region that, unfortunately, are too complex to assign; however, the IR spectrum of **7** is compatible with bidentate BH_4^- ligands as discussed above

Table V. Intraannular Torsion Angles (deg) with Standard Deviations in Parentheses

N(1)-Hf(1)-P(1)-C(1)	-48.6 (2)
Hf(1)-P(1)-C(1)-Si(1)	44.8 (3)
N(1)-Si(1)-C(1)-P(1)	-18.6 (4)
C(1)-Si(1)-N(1)-Hf(1)	-28.9 (4)
P(1)-Hf(1)-N(1)-Si(1)	44.4 (2)
N(1)-Hf(1)-P(2)-C(2)	-43.3 (3)
Hf(1)-P(2)-C(2)-Si(2)	43.4 (4)
N(1)-Si(2)-C(2)-P(2)	-22.8 (5)
C(2)-Si(2)-N(1)-Hf(1)	-19.3 (4)
P(2)-Hf(1)-N(1)-Si(2)	36.2 (3)
N(2)-Hf(2)-P(3)-C(3)	-8.4 (3)
Hf(2)-P(3)-C(3)-Si(3)	31.4 (5)
N(2)-Si(3)-C(3)-P(3)	-47.1 (5)
C(3)-Si(3)-N(2)-Hf(2)	43.4 (4)
P(3)-Hf(2)-N(2)-Si(3)	-20.8 (3)
N(2)-Hf(2)-P(4)-C(4)	28.5 (3)
Hf(2)-P(4)-C(4)-Si(4)	-37.1 (4)
N(2)-Si(4)-C(4)-P(4)	29.6 (5)
C(4)-Si(4)-N(2)-Hf(2)	-2.2 (4)
P(4)-Hf(2)-N(2)-Si(4)	-15.4 (3)

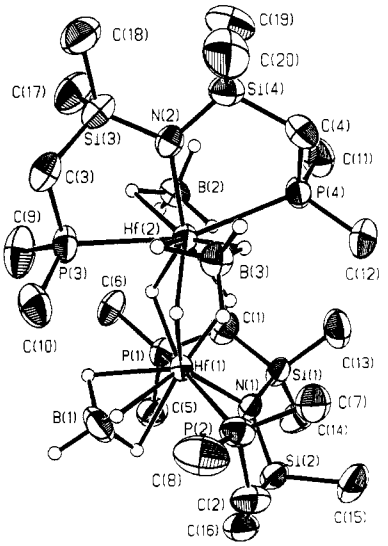

Figure 3. Single-crystal solid-state structure of $[Hf[N(SiMe_2CH_2PMe_2)_2]]_2(\mu\text{-}H)_3(BH_4)_3$ (**6**) and numbering scheme.

for **4**. The ^1H NMR resonances of the tridentate ligands in **6** (Figure 1) are consistent with a meridional (trans) bonding mode on each hafnium since virtual triplets[25] are again observed for both the methylene (PCH_2Si) protons and the phosphorus methyl protons. On the other hand, the ^1H NMR spectrum of the binuclear tetrahydride, **7**, is more complicated (Figure 2); the presence of two silylmethyl singlets, two virtual triplets for the phosphorus methyl protons, and two *coupled* multiplets for the methyl protons suggest a dimeric structure with equivalent ligands arranged in a meridional bonding mode but with the "top" and "bottom" of each ligand inequivalent.

It is difficult to unambiguously assign a structure for the binuclear trihydride **6** that embodies all of the pertinent data above. In particular, the presence of *three* BH_4^- ligands (binding mode unknown) on *two* hafnium centers necessarily requires an unsymmetrical structure; yet, the high symmetry of the ^1H NMR spectrum (Figure 1) is inconsistent with this datum. Not surprisingly, variable-temperature ^1H NMR studies on **6** indicate that there are fluxional processes occurring, since we observe broadening of all resonances as the temperature is lowered; however, no limiting low-temperature spectrum has been achieved even at −100 °C. The singlet observed in the $^{31}P\{^1H\}$ NMR spectrum of **6** also broadens as the temperature is lowered to give, at −50 °C, a complicated unsymmetrical pattern that we have not been able to analyze.

Fortunately, we were able to obtain X-ray-quality single crystals of **6**. The solid-state structure of this binuclear trihydride is shown

Scheme II

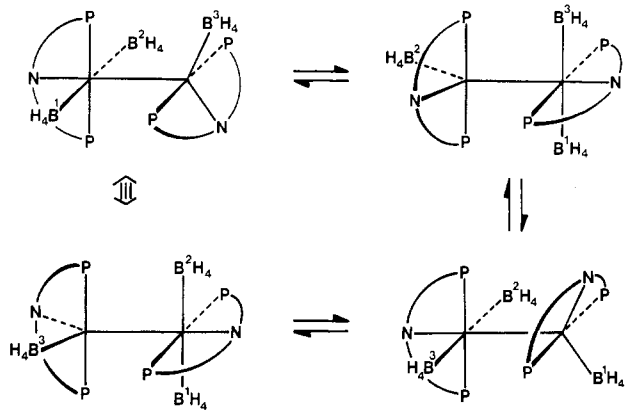

Scheme III

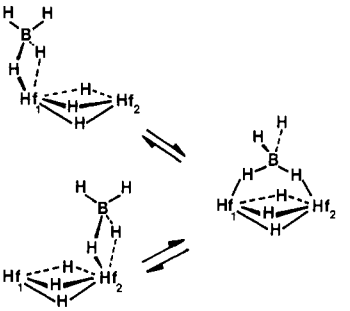

in Figure 3. The unsymmetrical, complicated geometry can be more simply represented as an idealized trigonal bipyramid at Hf(1) and an octahedron at Hf(2):

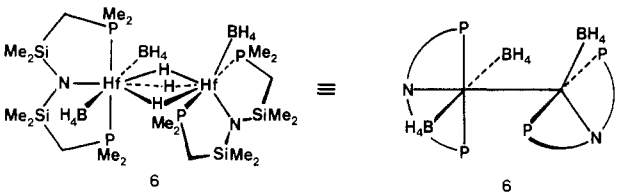

This simplified representation neglects the binding mode of the BH_4^- ligands and treats them as occupying a single coordination site, and similarily, the three bridging hydrides are considered as a vector joining the two geometries. Given this simple idealized geometry for **6**, what fluxional process can be invoked to explain the observed room-temperature ^1H and $^{31}P\{^1H\}$ NMR spectra? We propose that the BH_4^- ligands are being transferred intramolecularly from one hafnium to the other as shown in Scheme II. Interestingly, the process of moving BH_4^- ligands from the octahedral hafnium center, Hf(2), to the trigonal-bipyramidal hafnium site, Hf(1), results in the equilibration of the two ends of the dimer, and the "top" and the "bottom" of each individual ligand; in addition all the phosphine donors become equivalent if this process is fast on the NMR time scale. Thus this process alone can account for the spectroscopic data in the fast-exchange limit.

The intramolecular migration of a BH_4^- ligand from one metal to another has no precedent to our knowledge,[24] and therefore, just how this migration occurs is also not known. We believe that the bridging hydrides between the two hafnium centers are not intimately involved in the BH_4^- transfer (vide infra) but rather hold the two hafnium centers in proximity to facilitate a bridging BH_4^- interaction as shown in Scheme III. Unfortunately, bridging BH_4^- ligands via monodentate B–H interactions to each metal are not well established.[31]

(31) (a) Holah, D. G.; Hughes, A. N.; Hui, B. C. *Can. J. Chem.* **1975**, *53*, 3669. (b) Vites, J. C.; Eigenbrot, C.; Fehlner, T. P. *J. Am. Chem. Soc.* **1984**, *106*, 4633.

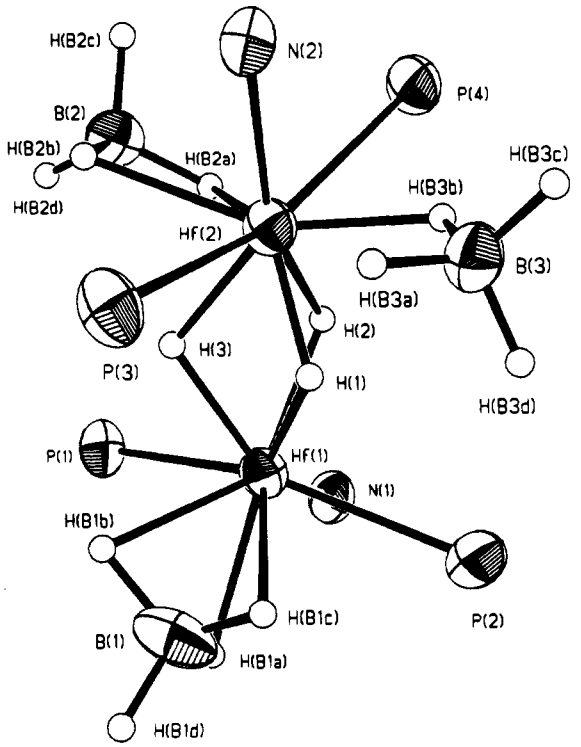

Figure 4. Detailed structure of **6** accurately depicting the coordination geometry at each hafnium center, the numbering scheme for all of the hydrides, and the bonding modes of the three BH_4^- units. The backbone of the ligands and the phosphorus substituents have been omitted for clarity.

The solid-state structure of **6** (Figure 3) clearly shows the presence of the three bridging hydrides between the hafnium centers. The Hf–H distances (Table III) are ~1.91–1.95 (6) Å with the exception of Hf(2)–H(1), which is ~0.2 Å shorter (not statistically significant). All of these distances are only slightly shorter than the 2.05-Å length reported for the binary hydride HfH_2.[32] The BH_4^- ligands on **6** are coordinated in a very unusual and unsymmetrical fashion; one BH_4^- unit is bound in a *tridentate* fashion to Hf(1), while the remaining two BH_4^- molecules are apparently bound in a *bidentate* mode to Hf(2). The average Hf–H_b distance of 2.25 Å of the symmetric triply bridged BH_4^- unit is longer than the analogous distance of 2.130 (9) Å found for $Hf(BH_4)_4$ by neutron diffraction.[33] Both of the bidentate BH_4^- ligands are bound asymmetrically to Hf(2) as has been observed[34] for $Hf(BH_4)_2(\eta^5\text{-}C_5H_4Me)_2$; however, while the Hf–$H_b$ distances of 2.01 and 2.25 Å to B(2) are indeed asymmetric, the corresponding Hf–H_b bond lengths of 1.93 and 2.43 Å to B(3) are so different that this BH_4^- ligand is best described as bound in a monodentate mode; this is more clearly shown in Figure 4. Thus the binuclear trihydride **6** contains all three possible hafnium–hydrogen–boron multicenter interactions:[24] monodentate (distorted), bidentate, and tridentate tetrahydroborate ligands. The Hf–B distances support this conclusion since they increase as the multicenter interactions decrease[33] (i.e. Hf(1)–B(1) = 2.322 (8) Å, Hf(2)–B(2) = 2.583 (6) Å, Hf(2)–B(3) = 2.636 (7) Å). The Hf(1)–N(1) bond distance of 2.176 (5) Å is very similar to other Hf–N bond distances reported but is shorter than the Hf(2)–N(2) distance of 2.264 (5) Å. The Hf–P bond lengths range from 2.712 (2) to 2.7859 (15) Å and are comparable to Hf–P distances found[10] in *fac*-$HfCl_3[N(SiMe_2CH_2PMe_2)_2]$ but are slightly longer than the Hf–P lengths reported[15c] for $Hf(\eta^4\text{-}C_4H_6)(Me_2PCH_2CH_2PMe_2)_2$.

Scheme IV

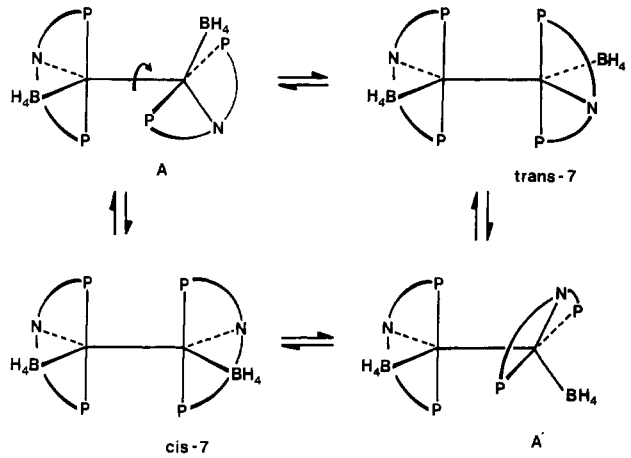

The bond angles (Table IV) more accurately reflect the geometry around each hafnium center. In particular the P–Hf–P angles of 149.57 (5) and 158.59 (5)° are noticeably less than the 180° angle required for the idealized representation of **6** above; however, we believe that due to the internal constraints of the two chelate rings of the tridentate ligand and the relatively long Hf–P bonds, a P–Hf–P bond angle of 180° is unattainable.[35] Our use of the term "meridional" is therefore only an approximation.

The details of the solid-state structure of **6**, as presented above, provide support for the proposed migration of BH_4^- ligand as shown in Scheme II. It is interesting that one of the BH_4^- units at the octahedral Hf(2) center appears to be bound in a monodentate fashion (Figure 4) since this is the required first step in BH_4^- ligand movement between metal centers. We believe that this piece of structural evidence provides support for the proposed BH_4^- migration process (Scheme II) even in the absence of a precedent.

Unfortunately, we have been unable to obtain X-ray-quality single crystals of the binuclear tetrahydride **7**. However, some of the conclusions reached above on the geometry and structure of the binuclear trihydride **6** can be applied to **7** to generate a reasonable model for its solution behavior. If one BH_3 is removed (as H_3BNMe_3) from the octahedral center of **6**, with concomitant formation of a fourth bridging hydride ligand, a simplified structure for **7** can be envisaged:

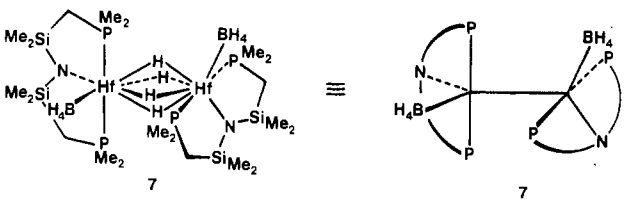

The geometry around both hafnium centers is idealized trigonal bipyramidal but with a 90° torsion angle relating each of the five coordinate geometries; again, the bidentate BH_4^- units (from IR analysis) are positioned at single coordination sites and the four bridging hydrides are represented as a vector joining the two hafnium centers. To account for the observed ^1H NMR spectrum, (Figure 2), we propose that intramolecular "rotations" about the hafnium–hafnium vector can occur as shown in Scheme IV.

A theoretical analysis[36] of this type of process suggests that "rotation" of one end of the dimer (Scheme IX) should be more facile than any process involving the bridging hydrides in motion around the hafnium–hafnium vector; in fact, the energy barrier

(32) Gibb, T. R. P., Jr.; Schumacher, D. P. *J. Phys. Chem.* **1960**, *64*, 1407.
(33) Broach, R. W.; Chuang, I.-S.; Marks, T. J.; Williams, J. M. *Inorg. Chem.* **1983**, *22*, 1081.
(34) Johnson, P. L.; Cohen, S. A.; Marks, T. J.; Williams, J. M. *J. Am. Chem. Soc.* **1978**, *100*, 2709.
(35) Compare, for example, the almost perfect "meridional" geometry found in $PdCl[N(SiMe_2CH_2PPh_2)_2]$, where the following bond lengths are pertinent: Pd–N = 2.063 (2) Å; Pd–P = 2.3078 (5), 2.3112 (5) Å (Fryzuk, M. D.; MacNeil, P. A.; Rettig, S. J.; Secco, A. S.; Trotter, J. *Organometallics* **1982**, *1*, 918).
(36) For a theoretical analysis of this type of process, see: Dedieu, A.; Albright, T. A.; Hoffmann, R. *J. Am. Chem. Soc.* **1979**, *101*, 3141.

to this "rotation" was calculated to be approximately 13–15 kcal mol^{-1}, which is remarkably close to our measured[37] value of 13.4 kcal mol^{-1}. Moreover, the proposed mechanism explains two important observations: (i) The ^{1}H NMR spectrum in the fast-exchange limit (ambient temperature) shows inequivalent environments above and below the ligand plane as would be predicted for each of the intermediates in Scheme IV; it should also be noted that both ends of every dimer in Scheme IV are equivalent (by internal comparison) with use of the appropriate symmetry operation. (ii) In the low-temperature limit, the ^{31}P{^{1}H} NMR spectrum of **7** shows an AB quartet due to inequivalent phosphorus donors; this can be accounted for by assuming that the thermodynamically most stable "rotational" isomer of **7**, and therefore the "rotamer" populated at low temperature, is the staggered dimer A (and A′) shown in Scheme IV, which, by symmetry, has inequivalent phosphorus atoms on each equivalent ligand. This type of "rotation" has been invoked previously[38] to explain the solution behavior of $[TaCl_2(PMe_3)_2]_2(\mu\text{-}H)_2$; interestingly, the related binuclear tetrahydride $[TaCl_2(PMe_3)_2]_2(\mu\text{-}H)_4$ is reported[38] to have a static structure.

A related binuclear tetrahydride complex of zirconium has been reported;[39] spectral analysis of $[ZrH(BH_4)(\eta^5\text{-}C_5Me_5)]_2(\mu\text{-}H)_2$ supports a formulation with bidentate BH_4^- units and both terminal and bridging hydrides. Variable-temperature ^{1}H NMR studies on the isoelectronic binuclear tetrahydride **7** provide no evidence for terminal hydrides since the bridging hydride resonance broadens as the temperature is lowered but no significant change in chemical shift is observed.[40] The absence of an IR band in the terminal M–H region (~1540–1650 cm^{-1} for M = Zr, Hf[39]) also supports only bridging hydrides in **7**. This comparison illustrates the remarkable influence of ancillary ligands ($C_5Me_5^-$ vs. $^-N(SiMe_2CH_2PMe_2)_2$) in determining the different stereochemistries in otherwise isoelectronic metal complexes.

The reaction of NMe_3 with the corresponding hafnium complex containing isopropyl substituents on phosphorus, $Hf(BH_4)_3[N(SiMe_2CH_2P(i\text{-}Pr)_2)_2]$ (**5**), does not result in BH_3 removal under any of the conditions we have tried; presumably, approach of NMe_3 to the BH_4^- ligands is impeded by the bulky diisopropylphosphine donors of the ancillary ligand.

Mechanistic Considerations. Our initial thoughts[28] on the formation of these binuclear mixed-hydride–tetrahydroborate derivatives, **6** and **7**, from the mononuclear precursor **4**, involved stepwise removal of BH_3 by the Lewis base with a dimerization at some point. The tendency for the formation of bridging hydrides with the group 4[44] metals, Zr and Hf, is well established,[5,7,39,41] and therefore, it is plausible to suggest that dimerization occurs *after* the *first* BH_3 cleavage (eq 4). A symmetrical binuclear

$$\underset{\mathbf{4}}{Hf(BH_4)_3[N(SiMe_2CH_2PMe_2)_2]} \xrightarrow[\text{(2) dimerization}]{\text{(1) } -BH_3\leftarrow L} \underset{\mathbf{8}}{[Hf(BH_4)_2[N(SiMe_2CH_2PMe_2)_2]]_2(\mu\text{-}H)_2} \quad (4)$$

complex that has *four* tetrahydroborate ligands and *two* bridging hydrides, as in **8**, is a likely intermediate since further cleavage of BH_3 from either end of the dimer **8** would lead directly to the binuclear trihydride **6**. We attempted to synthesize **8** unambiguously using methodology developed in our laboratory; to our surprise, we found that **8** is unstable and decomposes in a manner that is relevant to the formation of **6** and **7**.

Scheme V

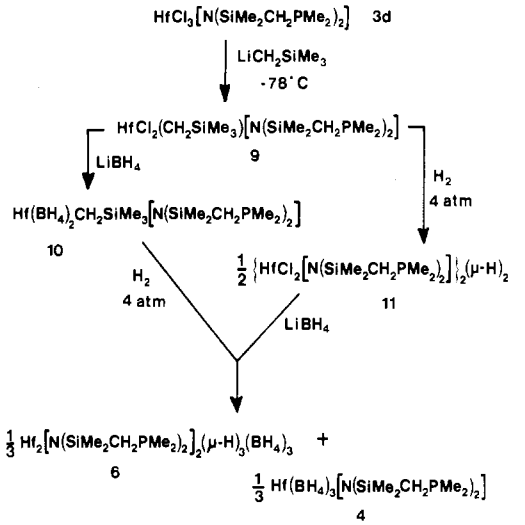

Scheme VI

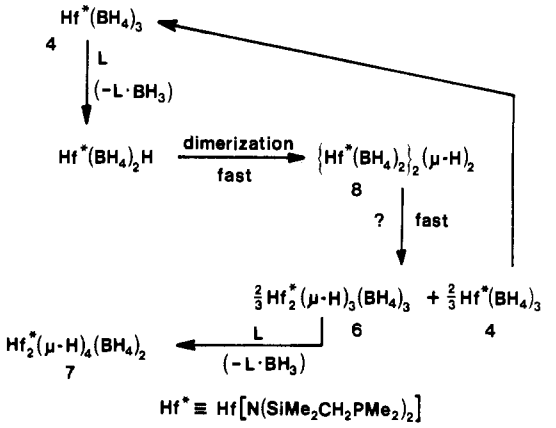

Treatment of the mono(ligand) starting material $HfCl_3[N(SiMe_2CH_2PMe_2)_2]$ (**3d**) with 1 equiv of $LiCH_2SiMe_3$ generates the monoalkyl derivative $HfCl_2(CH_2SiMe_3)[N(SiMe_2CH_2PMe_2)_2]$ (**9**), which is further transformed to the mononuclear bis(tetrahydroborate) complex **10** with excess $LiBH_4$. The monoalkyl derivative **9** can also be transformed into the binuclear dihydride **11** by direct reaction of hydrogen (4 atm) in toluene.[42] Attempts to generate **8** from **10** by hydrogenolysis, or from **11** by reaction with excess $LiBH_4$, as shown in Scheme V, only generated reproducible mixtures of the binuclear trihydride **6** and the mononuclear tris(tetrahydroborate) **4**. No other products were observed. Integration using both ^{1}H NMR and ^{31}P{^{1}H} NMR verifies the formation of equimolar amounts of the dimer **6** and **4**; mass balance requires the stoichiometry shown in Scheme V. Monitoring the reaction of the bis(tetrahydroborate) complex **10** with H_2 by ^{31}P{^{1}H} NMR only shows the gradual appearance of **6** and **4** at the expense of **10**; no peaks assignable to **8** were observed. Therefore, we conclude that **8** decomposes as rapidly as it forms to a mixture of **6** and **4** *without the necessity of a Lewis*-base-promoted BH_3 cleavage reaction; this rules out the initially proposed mechanism, which involved simple, stepwise BH_3 removal. Scheme VI summarizes these results. It is proposed (Scheme VI) that once the binuclear dihydride intermediate **8** is generated by BH_3 cleavage from **4** followed by dimerization, it rearranges to **6** and **4**; the latter complex **4** is recycled to further react with the Lewis base.

The most crucial step in the proposed mechanism (Scheme VI) is the decomposition of presumed **8** to **6** and **4**. In an effort to probe this transformation, we examined the reaction of the mo-

(37) ΔG^*_{280} = 13.4 kcal mol^{-1} was calculated by using the equation $\Delta G^*_{T_c} = -RT_c \ln(\pi(\Delta\nu)h/2^{1/2}kT_c)$, where T_c = coalescence temperature (280 K), $\Delta\nu$ = separation of the AB quartet (99.6 Hz), and the usual values obtain for the constants R, h, and k.

(38) Sattelberger, A. P. *ACS Symp. Ser.* **1983**, *No. 211*, 291 and references therein.

(39) Wolczanski, P. T.; Bercaw, J. E. *Organometallics* **1982**, *1*, 793.

(40) If the room-temperature hydride resonance of **7** was time averaged for terminal and bridging hydrides, then decreasing the temperature (lowering the rate of exchange of the two sites) should cause this signal to disappear and new resonances should appear at different chemical shifts (symmetrically disposed about the time-averaged chemical shift).

(41) Bercaw, J. E. In ref 3a, p 136.

(42) Discussions of stereochemistry and solution behavior of complexes **9**–**11** will be reported elsewhere.

Scheme VII

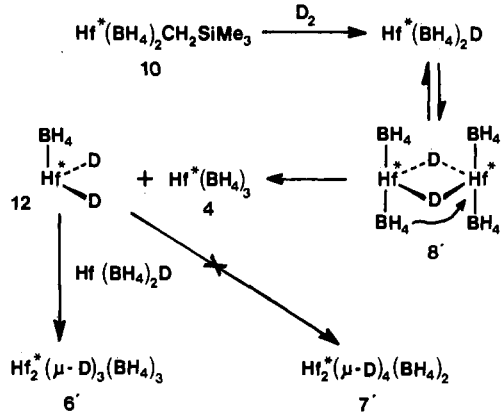

nonuclear bis(tetrahydroborate) complex **10** with D_2. By $^{31}P\{^1H\}$ NMR, the same distribution of **6** and **4** was obtained; however, the ^1H NMR spectrum indicated that **6** was fully deuterated in the bridging hydride positions (eq 5, Hf* = Hf[N-

$$\underset{\mathbf{10}}{Hf^*(BH_4)_2CH_2SiMe_3} \xrightarrow[4\text{ atm}]{D_2} Hf^*_2(\mu\text{-}D)_3(BH_4)_3 + \underset{\mathbf{4}}{Hf^*(BH_4)_3} \quad (5)$$

$(SiMe_2CH_2PMe_2)_2$]). Unfortunately, we were unable to determine[43] if any deuterium incorporation had occurred on the BH_4^- ligands of either **6** or **4**.

This apparently specific incorporation of deuterium can be rationalized (Scheme VII) if the initially formed binuclear dideuteride **8'** undergoes BH_4^- migration (cf. Scheme II) to fragment into the mononuclear dideuteride **12** and the tris(tetrahydroborate) complex **4**. The fate of **12** is speculation, but the observed deuterium specifity for the production of **6** suggests a recombination process with the mononuclear precursor to **8'**, $Hf^*(BH_4)_2D$ (Hf* ≡ Hf[N($SiMe_2CH_2PMe_2)_2$]). Simple dimerization of the intermediate **12** to generate **7'** (Scheme VII) can be excluded since none of this material is detected in any of these reactions.

The results of this deuteration experiment are also relevant to the pathway proposed for BH_4^- migration in **6** (Scheme III); the bridging deuterides of **6'** are clearly not involved in the process by which BH_4^- ligands are exchanged between hafnium centers since we observe no scrambling of hydrogen into the bridging positions from the BH_4^- groups as would be expected on the basis of the well-known[24] bridge to terminal B–H exchange process.

Conclusions

BH_3 cleavage from the mononuclear hafnium–tris(tetrahydroborate) complex **4** produces two new and unusual binuclear hydrides, **6** and **7**. The nonrigid behavior of these derivatives can be rationalized by invoking a novel intramolecular, intermetal BH_4^- migration in **6**, while for **7**, a "rotation" of the ends of the dimer satisfactorily explains the observed spectroscopic data.

The mechanism of formation of the binuclear complex **6** from the mononuclear precursor **4** has been probed by product analysis and deuteration studies. A simple, stepwise removal of BH_3 is not involved, but rather, a fragmentation–recombination process is likely to be operative.

It is significant that this ancillary ligand system promotes the formation of binuclear complexes which do not have analogues to derivatives that incorporate cyclopentadienyl type ligands. In particular, a binuclear zirconium complex,[39] which contains the $C_5Me_5^-$ ancillary ligand, adopts completely different types of binding modes for the hydride ligands than is found in the isoelectronic binuclear tetrahydride **7**, which is stabilized by the tridentate ligand $^-N(SiMe_2CH_2PMe_2)_2$. Further work on this type of ancillary ligand system coordinated to the early transition metals is in progress.

Acknowledgment. This work was supported by the Natural Sciences and Engineering Research Council of Canada. Thanks are due to Professor James Trotter for the use of his X-ray diffractometer and crystal structure solving programs.

Note Added in Proof. After submission of this manuscript, a paper by Bergman et al. reported the X-ray crystal structure of a bridging BH_4^- analogous to that proposed by us in Scheme III: Gilbert, T. M.; Hollander, F. J.; Bergman, R. G. *J. Am. Chem. Soc.* **1985**, *107*, 3508.

Registry No. **4**, 83634-66-6; **5**, 98720-53-7; **6**, 98720-54-8; **7**, 98720-55-9; **9**, 98720-56-0; **10**, 98720-57-1; **11**, 98720-58-2; $HfCl_3$[N($SiMe_2CH_2PMe_2)_2$], 98758-74-8; $HfCl_3$[N($SiMe_2CH_2P(i\text{-}Pr)_2)_2$], 94372-16-4; PMe_3, 594-09-2; NMe_3, 75-50-3.

Supplementary Material Available: Calculated coordinates and isotropic thermal parameters for the "organic" hydrogen atoms (Table VI), anisotropic thermal parameters (Table VII), torsion angles (Table VIII), a stereoview of refined borohydride H atom positions, and measured and calculated structure factor amplitudes (Table IX) (52 pages). Ordering information is given on any current masthead page.

(43) Both IR and ^2H NMR analyses were attempted, but no conclusive results were obtained.

(44) In this paper the periodic group notation is in accord with recent actions by IUPAC and ACS nomenclature committees. A and B notation is eliminated because of wide confusion. Groups IA and IIA become groups 1 and 2. The d-transition elements comprise groups 3 through 12, and the p-block elements comprise groups 13 through 18. (Note that the former Roman number designation is preserved in the last digit of the new numbering: e.g., III → 3 and 13.)

Contribution from the Departments of Chemistry, University of Southern California, Los Angeles, California 90089-1062, and University of Notre Dame, Notre Dame, Indiana 46556

Coordinated Hexafluoroantimonate: X-ray Crystal Structure of the Intermediate-Spin Iron(III) Tetraphenylporphinato Complex $Fe(TPP)(FSbF_5)\cdot C_6H_5F$

KENNETH SHELLY,[1] T. BARTCZAK,[2] W. ROBERT SCHEIDT,*[2] and CHRISTOPHER A. REED*[1]

Received May 30, 1985

In order to resolve inconsistencies in the literature concerning the spin state and structure of $Fe^{III}(TPP)(SbF_6)$ the X-ray crystal structure of (hexafluoroantimonato)(*meso*-tetraphenylporphinato)iron(III)–fluorobenzene, $Fe(TPP)(FSbF_5)\cdot C_6H_5F$, has been determined. Crystal data: orthorhombic, space group $Pna2_1$, $Z = 4$, $a = 25.754$ (6) Å, $b = 10.748$ (2) Å, $c = 15.707$ (4) Å, $\rho_{calcd} = 1.528$ g/cm^3, $\rho_{obsd} = 1.54$ g/cm^3. Diffraction data were collected by the θ–2θ scan method; all unique data to $2\theta \leq 66.8°$ were measured. A total of 6126 reflections were used in the structure determination; final discrepancy indices are $R_1 = 0.049$ and $R_2 = 0.057$. The complex is not ionic. The hexafluoroantimonate ligand is found to coordinate to iron in a monodentate fashion with an FeFSb bridge angle of 150.4 (2)° and an Fe–F bond length of 2.105 (3) Å. The short average Fe–N distance (1.978 (3) Å) and the small out-of-plane iron atom displacement are in accord with a nearly pure $S = {}^3/_2$ spin state.

The perchlorato complex $Fe(OClO_3)(TPP)$[3,4] is representative of a number of iron(III) porphyrins that have weak-field axial ligation.[5-12] A common feature of such complexes is their unusual admixed intermediate $S = {}^3/_2, {}^5/_2$ spin states, which give rise to

0020-1669/85/1324-4325$01.50/0